Comprehensive Analysis of Immune-Related Metabolic Genes in Lung Adenocarcinoma

FangFang Li
Zhengzhou University First Affiliated Hospital
Chun Huang
Zhengzhou University First Affiliated Hospital
LingXiao Qiu
Zhengzhou University First Affiliated Hospital
Ping Li
Zhengzhou University First Affiliated Hospital
guojun zhang (zgj@zzu.edu.cn)
The first affiliated hospital of Zhengzhou university https://orcid.org/0000-0001-8650-0847

Research article

Keywords: lung adenocarcinoma, immunotherapy, TCGA, metabolic

Posted Date: July 29th, 2021

DOI: https://doi.org/10.21203/rs.3.rs-753680/v1

Abstract

Purpose: The immunotherapy of lung adenocarcinoma has received more and more attention. Different immune cells can affect other metabolic genes and lifespan, and cell metabolism directly regulates immune cell functions. Therefore, it is crucial to explore the role of immune-related metabolic genes in lung adenocarcinoma.

Methods: This study screened and studied immune-related metabolic genes from three aspects. First of all, we divide them into three categories based on different immune characteristics and research immunity and clinical pathology. Secondly, we used LASSO regression analysis to screen the immune-related metabolic genes and constructed the clinical prediction model for the screened genes. Finally, we selected the intersection of immune metabolism genes highly expressed in tumor sites and immune metabolism genes that are negatively related to survival and obtained potential genes.

Results: We first identified immune-related metabolic genes and immune cells that may affect tumor progression in lung cancer. Then, through LASSO regression analysis, we screened out nine hub genes (TK1, TCN1, CAV1, ACMSD, HS3ST2, HS3ST5, AMN, ADRA2C, ACOXL) and constructed a prognostic model. Finally, through the screening of tumor-related immune metabolism genes, we obtained five hub genes (HMMR, PFKP, RRM2, TCN1 and TK1). Our qRT-PCR result also showed that RRM2 positively correlates with CDK2, CDK4, CDK6, CDK8.

Conclusion: We conduct a comprehensive analysis of the immune infiltration of the tumor microenvironment of lung cancer, and finally determined RRM2 as a promising immune metabolism checkpoint for lung adenocarcinoma based on the high correlation of RRM2 with immune cells and CDK family.

Introduction

Lung cancer is one of the most common causes of cancer-related mortality, with over 40% of lung adenocarcinoma cases (LUAD)[1, 2]. Lung adenocarcinoma (LUAD) contributes to the significant histologic type of lung cancer with an unfavorable 5-year survival rate of only 15%[3-5]. In the past few decades, although comprehensive treatments such as surgical resection, chemotherapy, radiotherapy, and targeted molecular therapy have been carried out in clinical practice, most patients with LUAD are usually diagnosed as advanced stage, so most patients' prognosis not effectively. Now, the relationship between cancer immunotherapy and tumor microenvironment and metabolism has gradually attracted people's attention. Therefore, a comprehensive understanding of the mechanism of immune-related metabolic genes involved in the occurrence and development of LUAD is essential to improve diagnosis and prognosis.

The tumor microenvironment (TME) is the cellular environment in which the tumor develops and closely related to the occurrence and development of tumors[6, 7]. TME generally includes inflammatory cells and stromal cells that infiltrate the tumor. Lymphocytes infiltrating tumor tissues have been discovered for

more than a hundred years. After 1960, people began to consider the relationship between immunity and prognosis [8]. It has been found that the infiltration of T cells (80%) in the majority of tumors is positively correlated with whether the tumor has metastasized [9]. Aberrant cellular metabolism is emerging as a novel therapeutic target, and the interplay between metabolic remodeling and immune regulation in cancer represents an active area of investigation[10, 11]. The abnormal metabolism of tumors not only enables tumors to survive in an environment of hypoxia and nutrient deficiency, but the products of metabolism can inhibit immune response, promote the formation of immunosuppressive cells, and help tumors evade host immune killing[12]. Mounting evidence has confirmed that reprogramming the tumor immune microenvironment is a necessary process that drives LUAD metastasis[13].

In this study, we downloaded the mRNA data of LUAD patients from the Cancer Genome Atlas (TCGA). Then we download metabolism-related genes from articles published by Peng, X[14], and immune-related genes from https://www.immport.org/. We first calculated the correlation between metabolic genes and immune genes, then enriched the immune-related metabolic genes and constructed protein interaction networks. In cancer and para-cancerous samples, the differences in immune-related metabolic genes are compared, and the different immune-related metabolic genes are functionally enriched. Because the enrichment analysis yielded different biological pathways, we further clustered the immune metabolism genes into a consistent cluster. According to the clustering results, we divided the immune metabolism genes into three clusters. We compared the level of immune cell infiltration, immune score, and clinicopathological information between different clusters. By constructing a predictive model, we determined that low expression of immune-related metabolic genes is related to better survival prognosis. Finally, we took the intersection of the highly expressed genes at the tumor site and the immune metabolism genes negatively related to survival and identified five potential targets. Through the pan-cancer analysis of 5 genes, three genes with high expression abundance in tumors and negatively correlated with immune cells were screened: RRM2, TK1, HMMR. And based on the correlation with immunity, the results show that RRM2 gene has a positive correlation with CDK family genes. This result proves that the RRM2 has an undeniable role in predicting tumor immunotherapy and provides a promising support target for LUAD's future immunotherapy.

Materials And Methods

Data download and preprocessing

The mRNA sequencing and clinical data of 509 LUAD samples and 20 normal samples were downloaded from the TCGA data portal. Then we download metabolism-related genes from articles published by Peng, X[14], and immune-related genes from https://www.immport.org/. We normalized all data to log2 (tpm+1) and removed low-expressed immune genes and metabolic genes (average expression after normalization <0.5). Finally, through Spearman correlation calculation, 346 immune-related metabolic genes were screened out ($P<0.05$, $|R|>0.2$).

GO and KEGG Enrichment Analysis and PPI Network Construction of immune-related metabolic genes

We divided 346 DEGs into up-regulated genes and down-regulated genes and used R to perform GO and KEGG enrichment analysis. The “clusterProfiler”, “richplot”, and “ggplot2” packages are used for analysis[15, 16]. The GO analysis was performed to annotate genes and classify upregulated and downregulated DEGs. The GO terms consisted of 3 parts: Biological Process (BP), Cellular Component (CC), and Molecular Function (MF). The KEGG database includes the systematic analysis, annotation, and visualization of gene functions[17]. We use the STRING online website to construct a protein interaction network for the selected DEGs[18]. For PPI analysis, the confidence score is set to > 0.9, and only terms with both p- and q-value of <0.05 were considered significantly enriched. Cytoscape software further analysed the most closely connected modules and identified the top 10 central genes[19]. Next, we analyzed the differences in immune metabolism genes between cancerous tissues and adjacent tissues. The “limma” package[20] in R was used to identify DEGs between Cancer and adjacent tissue samples. Merely genes with | log2fold change | > 1 and P < 0.05 were considered as DEGs. The “pheamap” package is used to draw heat maps, and “ggplot2” is used to draw volcano maps.

Part 1: Immune characteristics and Molecular characteristics of immune-related metabolic genes.

Consistent clustering of immune-related metabolic genes

We divide immune-related metabolic genes into different clusters by the method of cell consistency clustering. We used the "ConsensusClusterPlus" package (100 iterations and 80% resampling rate, http://www.bioconductor.org/) to classify patients with LUAD into different subtypes. The heat map and dela diagram established the optimal number of clusters. Plot the cumulative distribution function (CDF) to identify the number of best clusters. Then we compared Progress Free Survival (PFS) between various clusters. The survival analysis was analyzed by R package “survival”, and the "ggplot2" package is used for plotting.

Immune characteristics between clusters-expression of immune-related molecules

Next, we analyzed immune-related molecules' expression among these clusters with the ESTIMATE algorithm through the R “ESTIMATE” package. These immune-related molecules regulate four immune functions, include antigen presentation, chemokine-related genes, cytokines and immune checkpoints. “ggplot2” package is used to draw box plots.

Immune characteristics between clusters-expression of infiltrating immune cells and clinicopathological characteristics

We used four methods, single sample gene set enrichment analysis (ssGSEA), Microenvironment Cell Populations (MCP)-counter, CIBERSORT, and Xcell[21-24], to assess the infiltration of immune cells in 3 clusters. Besides, we compared three different immune cell infiltrating clusters and reached their immune score. The pathological classification proportions between different cluster clusters were compared to further distinguish the differences between different clusters, including T, N, M, clinical drug treatment response, and the pathological stage.

Part 2: Validation of prognostic prediction based on models of immune-related metabolic genes

We first randomly divide the expression matrix of LUAD into a training set and a test set, with 70% of the training set and 30% of the test set. A single factor analysis was performed on the two groups of genes, and genes with p<0.05 were selected. The Least Absolute Shrinkage and Selection Operator (LASSO) cox regression method is an advanced dimensionality reduction algorithm that can help us determine the best number of genes to build a model[25, 26]. Then it is further optimized through multi-factor COX regression analysis. Finally, the gene's risk score is screened to have a good predictive ability on the patient's survival. The area under the ROC curve (AUC) is used to judge the prognostic model's predictive power. The ten-fold cross-validation based on “glmnet” package in R was used for lasso penalty Cox regression analysis. The survival analysis was analyzed by R package “survival”, while AUC was analyzed by R package “survivalROC”.

Part 3: Identify potential metabolic checkpoints and qRT-PCR validation

Identify potential metabolic checkpoints

Finally, we explored those immune-related metabolic molecules that can be used as metabolic checkpoints to provide a theoretical basis for future treatment. We first selected the immune metabolism genes that are highly expressed in the tumor site (logFC>1.5, FDR<0.05), and the immune metabolism genes that are negatively related to survival (this is the genes in the survival model training set), and then got five potential genes. Through pan-cancer analysis of five genes (https://cistrome.shinyapps.io/timer/), we screened out genes with higher expression abundance in tumors.

Quantitative real-time PCR (qRT-PCR)

Total RNA was extracted from lung cancer samples using TrIzol reagent (Invitrogen, Carlsbad, California) according to the manufacturer’s protocols, which was reverse transcribed into cDNA using a reverse transcription kit (Takara, Dalian, China). Next, qRT-PCR was performed using the SYBR-Green PCR kit (Roche Diagnostics, Indianapolis, IN) on a StepOnePlus Real-Time PCR system (Applied Biosystems, Foster City, CA). Glyceraldehyde 3-phosphate dehydrogenase (GAPDH) was used as internal control. The results were calculated using the 2-ΔΔCtmethod. Primers for qRT-PCR were synthesized by Sangon Biotech (Shanghai, China), and the sequences are listed in Supplementary Table 1.

Results

Screening of immune-related metabolic genes

We obtained 1041 immune-related genes and 1613 metabolic-related genes from the Online website. Then we got 346 immune-related metabolic genes by Spearman correlation calculation.

GO and KEGG Enrichment Analysis and PPI Network Construction of immune-related metabolic genes

The GO enrichment and KEGG pathway analyses of the 346 immune-related metabolic genes were conducted using “clusterProfiler” package in the R environment. As mentioned earlier, the GO analysis results consisted of three parts: BP, CC, and MF. The results indicated that the Immune-related metabolic genes were significantly enriched in the BP-associated organic acid biosynthetic process, carboxylic acid biosynthetic process and monocarboxylic acid biosynthetic process. For the CC, the immune-related metabolic genes were mainly enriched in the Golgi lumen, lysosomal lumen, and vacuolar lumen. Furthermore, through the MF analysis, it was found that the immune-related metabolic genes were notably enriched in cofactor binding, oxidoreductase activity, acting on the CH–OH group of donors and carboxylic acid-binding. KEGG was used to analyze the signaling pathways that immune-related metabolic gene enrichment. Immune-related metabolic genes were enriched in Arachidonic acid metabolism, PPAR signaling pathway, and Biosynthesis of amino acids (Figure 1A-1B). To further explore its potential mechanism, we use Cytoscape software [National Institute of General Medical Sciences (NIGMS)] to build a PPI network (confidence level = 0.9) (Figure 1C) based on the STRING database. Then we identified the core genes of top10 through the Cytoscape plug-in cytoHubba: SDC2, GPC3, GPC1, HSPG2, AGRN, GPC2, GPC5, GPC4, GPC6, VCAN (Figure 1D). Then we further analyzed the differences between immune-related metabolic genes in cancer and para-cancerous tissues. As shown in Supplementary Figure 1, the heat map clearly distinguishes the LUAD samples from adjacent tissue samples (Figure S1A). A total of 141 DEGs were identified (| log2fold change |> 1, $P<0.05$), including 72 upregulated and 69 downregulated genes (Figure S1B). Then, we performed GO and KEGG enrichment analysis on 141 differential genes (Figure S1C-S1F). The function enrichment of DEGs is mainly concentrated in: fast acid metabolic process; organic hydroxy compound metabolic process; small molecular metabolic process.

Part 1: Immune characteristics and Molecular characteristics of immune-related metabolic genes.

Consistent clustering of immune-related metabolic genes

We already know that immune metabolism genes regulate different biological pathways through the previous research results, speculating that various tumors will have different metabolic methods and show other biological characteristics. We clustered the immune-related metabolic genes in a consistent cluster to explore the metabolic patterns of tumor cells. We can divide tumor samples into different clusters according to different immune infiltration results through cell clustering. Plot the cumulative distribution function CDF to identify the number of optimal clusters (Figure 2A-2B). And then, we identified three different clusters and drew heat maps to compare the expression of immune-related metabolic genes among the various clusters (Figure 2C). The results showed that cluster2 had the best immune cell infiltration, followed by cluster3 and cluster1. In the end, we evaluate the survival status of the three clusters. By comparing progression-free survival (PFS), it can be found that cluster2 has a better survival rate (Figure 2D).

Immune characteristics between clusters-expression of immune-related molecules

We further analyzed the expression of immune-related molecules among these clusters. We analyze the **molecules** correlated with antigen-presentation (B2M, HLA-A, HLA-B, HLA-C, HLA-DPA1, HLA-DQA1, TAP1, TAP2), chemokine-related genes (CCL4, CCL5, CXCL10, CXCL13, CXCL9), immune checkpoint molecules (CD226, CD274, CD276, CD40, CTLA4, HAVCR2, LAG3, PDCD1) and cytokines (GZMB, GZMH, IFNG, IL2, PRF1, TNF) expressions by drawing a box plot for comparison (Figure 3A-3D). We found that different clusters have different immune functions. There are apparent differences between them, and there is no complete consistency. In Antigen, we found that HLA-DPA1 and HLA-DQA1 have the highest expression levels in cluster2. Chemokine found that CXCL13 is a higher expression level in cluster2. The immune checkpoints showed that CD226 and CTLA4 had higher expression levels, and IL2 also increased significantly. The differences in these immune-related genes may help explain the better survival status of patients in cluster2.

Immune characteristics between clusters-expression of infiltrating immune cells and clinicopathological characteristics

We use the four reported methods (ssGSEA, MCP-counter, CIBERSORT, and Xcell) to evaluate these three clusters' immune cell infiltration level. We explored two aspects: immune effector cells (Figure4A-4D) and immunosuppressive cells (Figure4E-G). It can be seen that in general, cluster1 had the least infiltration of immune effector cells and immunosuppressive cells, suggesting that cluster1 might be the immunologically-cold tumors, while cluster 2 and cluster 3 were enriched by both immune effector cells and immunosuppressive cells, which might suggest that both cluster 2 and cluster 3 had immunologically-hot tumor immune microenvironments. In cluster2, the content of activated B cells, DC, and monocytes was significantly increased. Finally, we compared three different immune cell infiltrating clusters and reached their immune score (Figure4H). The results show that cluster2 has a higher immune score and stromal score. Besides, we compare the different clinicopathological parameters between the clusters, including tumor stage, TNM classification and drug response. As shown in Figure S2, we found that different clusters are significantly related to the TNM staging of diabetes. In cluster 2, the patients with stage III and IV is significantly lower than that in stage I and II (A-C). In terms of lymph node metastasis, the proportion of non-metastatic patients is highest in cluster2 (D-F), and the lowest in cluster1; also, in terms of distant metastasis of tumor, tumor stage and drug response, patients in cluster2 have better performance (G-O).

Part 2: Validation of prognostic prediction based on models of immune-related metabolic genes

LASSO COX regression analysis

Next, we explore whether these immune metabolism genes have the function of predicting survival. To achieve this goal, we randomly divide the LUAD matrix into a training set and a test set (70% of the training set and 30% of the test set). First, perform single factor analysis, select a total of 80 genes with $p<0.05$, These significant genes entered into LASSO COX regression analysis, and the regression coefficient was computed (Figure 5A-B). After selecting the best combination, use multivariate regression, select $p<0.05$ as the gene for constructing predictive models. The distributions of risk score of LUAD

patients and the relationships between risk score and survival time were visualized in Figure 5C-F. Finally, nine genes were identified: TK1, TCN1, CAV1, ACMSD, HS3ST2, HS3ST5, AMN, ADRA2C, ACOXL.

Construct prognostic prediction models of immune-related metabolic genes

First, we perform single-factor COX analysis based on the hub genes (Figure 6A). In the training set and test set, patients were divided into high-risk and low-risk groups. According to the two groups of patient's clinical information, a survival curve was drawn (Figure 6B&6D). The results in the training set and test Focus on high score patients had a worse Overall Survival (OS) than those of low score patients ($p < 0.0001$). The area under the ROC curves (Area Under Curve: AUC) of the predictive model for LUAD has the same performance in the first year, third year and fifth year (Test set: AUC at one year: 0.68, AUC at three years: 0.76, AUC at five years: 0.61; Training set: AUC at one year: 0.83, AUC at three years: 0.72, AUC at five years: 0.71) (Figure 6C&6E).

Part 3: Identify potential metabolic checkpoints

Finally, we discussed that immune-related metabolic molecules could be used as a metabolic checkpoint to provide the theoretical basis for future treatment. To achieve this goal, we first selected high expression immune metabolic genes ($logFC > 1.5$, $FDR < 0.05$) in the tumor site because the high level of genes in the tumor may be a potential factor to promote tumor growth. In addition, we obtained five potential targets, HMMR, PFKP, RRM2, TCN1 and TK1(supplementary figure S3), by taking the cross points of immune metabolism genes negatively correlated with survival rate (these are the genes in the survival model training set). By comparing the survival rate of five hub genes in Pan-cancer and their relationship with immunity, it was confirmed that the RRM2 gene was highly correlated with immunity (supplementary figure S4&S5). Finally, we analyzed the correlation between the RRM2 gene and the CDK family, and the results show that these genes are highly correlated (Fig. 7C). These were also consistent with the results analyzed in the tumor samples by qRT-PCR (Figure 7D-G).

Discussion

As the most common cause of cancer-related deaths worldwide, lung adenocarcinoma seriously affects people's healthy lives. For a long time, surgery and adjuvant chemotherapy have been the most commonly used treatment methods. As patients gradually increase their willingness to live longer and further improve their quality of life, it is crucial to find new treatment options. As a new therapy, immunotherapy has gradually played an increasingly important role in treating various cancers. Abnormal cell metabolism is becoming a new therapeutic target, and the interaction between metabolic remodeling and immune regulation in cancer is an active area of research. Therefore, this study analyzed the sequencing samples of LUAD patients in TCGA, screened the immune-related metabolism genes of LUAD, and explored its mechanism in three parts, which provides theoretical support for the immunotherapy of LUAD.

This study downloads metabolism-related genes from articles published by Peng, X, and immune-related genes from https://www.immport.org/. We got the immune-related genes, Metabolic genes, enrichment analysis, and protein mutual aid network construction by taking the intersection. We first identified ten hub genes, SDC2, GPC3, GPC1, HSPG2, AGRN, GPC2, GPC5, GPC4, GPC6, and VCAN. Existing studies have shown that these genes play an essential role in the immune-related mechanisms of a variety of cancers (colorectal cancer[27], cervical cancer[28], liver cancer[29], pancreatic cancer[30] etc.).Existing studies have proved that the tumor microenvironment infiltration of tumor-infiltrating lymphocytes (TILs) is closely related to immunotherapy effectiveness [31]. Immune infiltration of tumor microenvironment in glioblastoma multiforme [32], breast cancer [33], lung cancer [34] It plays a vital role in immunotherapy, and the increase in the degree of immune infiltration is related to better immunotherapy effect.

First, we explored the specific mechanisms of these immune-related metabolic genes. The samples were divided into three clusters through consistent clustering, and then the levels of immune cell infiltration, immune scores, and clinicopathological information were compared. We found that in cluster2, the expression of HLA-DPA1 was the highest. HLA-DPA1, belongs to the HLA class II alpha chain paralogues[35], participate in immune response and antigenic peptides presentation. Existing studies have shown that the down-regulation of HLA-DPA1 expression is related to the poor prognosis of tumors[36-38]. HLA-DQA1, which is one of the MHC Class II family members, may be a potential prognostic biomarker for ESCC[39]. We found that in cluster2, the chemokine ligand 13 (CXCL13) gene expression was the highest. The tumor microenvironment includes stromal cells and tumor cells, and they interact through complex mutual interferences. These mutual interferences are mediated by a variety of growth factors, cytokines and chemokines. CXCL13 and its chemokine receptor 5 (CXCR5) are key chemokines that play a crucial role in chemotactic cancer cell biology. The CXCL13/CXCR5 signal axis plays a vital role in the occurrence and development of several human cancers[40]. Besides, in cluster2, the degree of activated B cells, DC, and monocytes infiltration were the highest, and the prognosis was better than the other two groups. The pathways related to B cells and B cells have played an important role in tumor immunotherapy[41]. It has been discovered that the controlled interaction between metabolism, extracellular stimuli and intracellular signaling can complete the experiential response. And this balance change can promote the malignant transformation of B cells[42]. Immunotherapy using dendritic cell (DC)-based vaccination is a generally accepted method in recent years. Similarly, monocytes also play an important role in antigen presentation in the microenvironment of tumor immune infiltration[43]. The critical role of immune-related metabolic genes and immune cells in cancer is gradually being unveiled[44].

Second, we identified nine genes TK1, TCN1, CAV1, ACMSD, HS3ST2, HS3ST5, AMN, ADRA2C, and ACOXL and constructed a prediction model. In the prediction of cancer, TK1[45, 46] has shown a significant effect. TCN1[47], CAV1 [48], HS3ST2[49] etc., play an essential role in the prediction and pathogenesis of a variety of cancers. TK1 and TCN1 have played a vital role in immune-related metabolism[50, 51]. Caveolin-1 (CAV1) 's primary functions include participation in endocytosis, cell signal tandem and tandem-mediated resonance of cell membrane invasion, and a critical correlation with lymphocyte infiltration[52].

Finally, we identified the metabolic checkpoints of LUAD. Through the intersection of highly expressed genes in tumors and immune metabolism genes negatively related to survival, we have obtained five potential metabolic checkpoints HMMR, PFKP, RRM2, TCN1, TK15. In pan-cancer, comparing their expression levels between cancers and their relationship with immune cells, we determined the critical role of RRM2 in lung adenocarcinoma. The recognized function of Ribonucleotide Reductase Small Subunit M2 (RRM2) is to maintain the balance of the dNTP pool for DNA synthesis and DNA repair. In breast cancer, RRM2 overexpression in cancer cells promotes the formation and invasion of 3D colonies[53]. In liver cancer[54], RRM2 can inhibit hypertrophy by stimulating GSS to synthesize GSH. In lung adenocarcinoma, RRM2 has been determined to have an independent prognostic significance[55]. Finally, we further explored the high correlation between RRM2 and the CDK family. Recent studies have shown that Cyclin-dependent kinases 4 and 6 (CDK4/6) inhibitors can regulate anti-tumor immunity. As the basic driving factor of the cell cycle, CDK4/6 is necessary for the occurrence and development of various malignant tumors. CDK4/6 inhibitors can significantly inhibit the proliferation of regulatory T cells[56]. Our research further confirms the relationship between the RRM2 gene and immunity and metabolism in lung adenocarcinoma and provides theoretical support for exploring the immunotherapy of LUAD.

Conclusion

In this study, we first identified the vital role of immune-related metabolic genes in lung adenocarcinoma's immune and clinicopathological aspects. Secondly, we constructed and validated the prediction models of TK1、TCN1、CAV1、ACMSD、HS3ST2、HS3ST5、AMN、ADRA2C and ACOXL. Finally, we screened RRM2 as a possible metabolic checkpoint of lung adenocarcinoma and explored the close relationship between RRM2 and CDK family. This result is helpful for the study of immunotherapy and immune-related metabolic genes in lung adenocarcinoma.

Abbreviations

TCGA: The Cancer Genome Atlas

KEGG: Kyoto Encyclopedia of Genes and Genomes

GO: Gene Ontology

DEGs: differentially expressed genes

LUAD: Lung adenocarcinoma

ssGSEA: single sample gene set enrichment analysis

TME: tumor microenvironment

PPI: protein-protein interaction

Declarations

Funding: No funding

Conflict of Interest Statement

The authors declare no conflict of interest.

Acknowledgments

We thank the TCGA program for the RNA-sequence and clinical data of patients with lung adenocarcinoma.

Ethics Statement

Lung cancer tissue specimens were obtained from the First Affiliated Hospital of Zhengzhou University. The ethics committee of the First Affiliated Hospital of Zhengzhou University approved the study (Ethics number: 2020-KS-HNSR188). All the related patients have signed informed consent.

Availability of data and material

The data of this study are from the TCGA database.

Code availability

All analyses were performed using R version 3.6.3.

Authors' Contributions

LFF: Conceptualization of the study.

HC and QLX: Analyzed the data.

LP: Drafted the manuscript.

ZGJ: Guided on the quality of the research.

All authors read and approved submission of the final manuscript.

Ethics approval

Lung cancer tissue specimens were obtained from the First Affiliated Hospital of Zhengzhou University. The ethics committee of the First Affiliated Hospital of Zhengzhou University approved the study (Ethics number: 2020-KS-HNSR188). All the related patients have signed informed consent.

Consent to participate

Informed consent was obtained from all individual participants included in the study.

Consent to publish

The participant has consented to the submission of the case report to the journal.

References

1. Jordan EJ, Kim HR, Arcila ME, Barron D, Chakravarty D, Gao J, et al. **Prospective Comprehensive Molecular Characterization of Lung Adenocarcinomas for Efficient Patient Matching to Approved and Emerging Therapies**. *Cancer Discov* 2017; 7(6):596-609.
2. Siegel RL, Miller KD, Jemal A. **Cancer statistics, 2019**. *CA Cancer J Clin* 2019; 69(1):7-34.
3. Ferlay J, Colombet M, Soerjomataram I, Mathers C, Parkin DM, Pineros M, et al. **Estimating the global cancer incidence and mortality in 2018: GLOBOCAN sources and methods**. *Int J Cancer* 2019; 144(8):1941-1953.
4. Cancer Genome Atlas Research N. **Author Correction: Comprehensive molecular profiling of lung adenocarcinoma**. *Nature* 2018; 559(7715):E12.
5. Cancer Genome Atlas Research N. **Comprehensive molecular profiling of lung adenocarcinoma**. *Nature* 2014; 511(7511):543-550.
6. Wood SL, Pernemalm M, Crosbie PA, Whetton AD. **The role of the tumor-microenvironment in lung cancer-metastasis and its relationship to potential therapeutic targets**. *Cancer Treat Rev* 2014; 40(4):558-566.
7. Quail DF, Joyce JA. **Microenvironmental regulation of tumor progression and metastasis**. *Nat Med* 2013; 19(11):1423-1437.
8. Maccarty WC. **Longevity in Cancer: A Study of 293 Cases**. *Ann Surg* 1922; 76(1):9-12.
9. Husby G, Hoagland PM, Strickland RG, Williams RC, Jr. **Tissue T and B cell infiltration of primary and metastatic cancer**. *J Clin Invest* 1976; 57(6):1471-1482.
10. Buck MD, Sowell RT, Kaech SM, Pearce EL. **Metabolic Instruction of Immunity**. *Cell* 2017; 169(4):570-586.
11. Kesarwani P, Kant S, Prabhu A, Chinnaiyan P. **The interplay between metabolic remodeling and immune regulation in glioblastoma**. *Neuro Oncol* 2017; 19(10):1308-1315.
12. Biswas SK. **Metabolic Reprogramming of Immune Cells in Cancer Progression**. *Immunity* 2015; 43(3):435-449.
13. Lou Y, Diao L, Cuentas ER, Denning WL, Chen L, Fan YH, et al. **Epithelial-Mesenchymal Transition Is Associated with a Distinct Tumor Microenvironment Including Elevation of Inflammatory Signals and Multiple Immune Checkpoints in Lung Adenocarcinoma**. *Clin Cancer Res* 2016; 22(14):3630-3642.
14. Peng X, Chen Z, Farshidfar F, Xu X, Lorenzi PL, Wang Y, et al. **Molecular Characterization and Clinical Relevance of Metabolic Expression Subtypes in Human Cancers**. *Cell Rep* 2018; 23(1):255-269 e254.

15. Yu G, Wang LG, Han Y, He QY. **clusterProfiler: an R package for comparing biological themes among gene clusters**. *OMICS* 2012; 16(5):284-287.
16. Harris MA, Clark J, Ireland A, Lomax J, Ashburner M, Foulger R, et al. **The Gene Ontology (GO) database and informatics resource**. *Nucleic Acids Res* 2004; 32(Database issue):D258-261.
17. Ogata H, Goto S, Sato K, Fujibuchi W, Bono H, Kanehisa M. **KEGG: Kyoto Encyclopedia of Genes and Genomes**. *Nucleic Acids Res* 1999; 27(1):29-34.
18. von Mering C, Huynen M, Jaeggi D, Schmidt S, Bork P, Snel B. **STRING: a database of predicted functional associations between proteins**. *Nucleic Acids Res* 2003; 31(1):258-261.
19. Shannon P, Markiel A, Ozier O, Baliga NS, Wang JT, Ramage D, et al. **Cytoscape: a software environment for integrated models of biomolecular interaction networks**. *Genome Res* 2003; 13(11):2498-2504.
20. Diboun I, Wernisch L, Orengo CA, Koltzenburg M. **Microarray analysis after RNA amplification can detect pronounced differences in gene expression using limma**. *BMC Genomics* 2006; 7:252.
21. Newman AM, Liu CL, Green MR, Gentles AJ, Feng W, Xu Y, et al. **Robust enumeration of cell subsets from tissue expression profiles**. *Nat Methods* 2015; 12(5):453-457.
22. Barbie DA, Tamayo P, Boehm JS, Kim SY, Moody SE, Dunn IF, et al. **Systematic RNA interference reveals that oncogenic KRAS-driven cancers require TBK1**. *Nature* 2009; 462(7269):108-112.
23. Becht E, Giraldo NA, Lacroix L, Buttard B, Elarouci N, Petitprez F, et al. **Estimating the population abundance of tissue-infiltrating immune and stromal cell populations using gene expression**. *Genome Biol* 2016; 17(1):218.
24. Aran D, Hu Z, Butte AJ. **xCell: digitally portraying the tissue cellular heterogeneity landscape**. *Genome Biol* 2017; 18(1):220.
25. Friedman J, Hastie T, Tibshirani R. **Regularization Paths for Generalized Linear Models via Coordinate Descent**. *J Stat Softw* 2010; 33(1):1-22.
26. Sauerbrei W, Royston P, Binder H. **Selection of important variables and determination of functional form for continuous predictors in multivariable model building**. *Stat Med* 2007; 26(30):5512-5528.
27. Han YD, Oh TJ, Chung TH, Jang HW, Kim YN, An S, et al. **Early detection of colorectal cancer based on presence of methylated syndecan-2 (SDC2) in stool DNA**. *Clin Epigenetics* 2019; 11(1):51.
28. Hu R, Zhu Z. **ELK1-activated GPC3-AS1/GPC3 axis promotes the proliferation and migration of cervical cancer cells**. *J Gene Med* 2019; 21(8):e3099.
29. Fu J, Wang H. **Precision diagnosis and treatment of liver cancer in China**. *Cancer Lett* 2018; 412:283-288.
30. Melo SA, Luecke LB, Kahlert C, Fernandez AF, Gammon ST, Kaye J, et al. **Glypican-1 identifies cancer exosomes and detects early pancreatic cancer**. *Nature* 2015; 523(7559):177-182.
31. Chen DS, Mellman I. **Oncology meets immunology: the cancer-immunity cycle**. *Immunity* 2013; 39(1):1-10.

32. Sokratous G, Polyzoidis S, Ashkan K. **Immune infiltration of tumor microenvironment following immunotherapy for glioblastoma multiforme**. *Hum Vaccin Immunother* 2017; 13(11):2575-2582.
33. Burugu S, Asleh-Aburaya K, Nielsen TO. **Immune infiltrates in the breast cancer microenvironment: detection, characterization and clinical implication**. *Breast Cancer* 2017; 24(1):3-15.
34. Liu X, Wu S, Yang Y, Zhao M, Zhu G, Hou Z. **The prognostic landscape of tumor-infiltrating immune cell and immunomodulators in lung cancer**. *Biomed Pharmacother* 2017; 95:55-61.
35. Diaz G, Amicosante M, Jaraquemada D, Butler RH, Guillen MV, Sanchez M, et al. **Functional analysis of HLA-DP polymorphism: a crucial role for DPbeta residues 9, 11, 35, 55, 56, 69 and 84-87 in T cell allorecognition and peptide binding**. *Int Immunol* 2003; 15(5):565-576.
36. Rimsza LM, Roberts RA, Miller TP, Unger JM, LeBlanc M, Braziel RM, et al. **Loss of MHC class II gene and protein expression in diffuse large B-cell lymphoma is related to decreased tumor immunosurveillance and poor patient survival regardless of other prognostic factors: a follow-up study from the Leukemia and Lymphoma Molecular Profiling Project**. *Blood* 2004; 103(11):4251-4258.
37. Meissner M, Konig V, Hrgovic I, Valesky E, Kaufmann R. **Human leucocyte antigen class I and class II antigen expression in malignant fibrous histiocytoma, fibrosarcoma and dermatofibrosarcoma protuberans is significantly downregulated**. *J Eur Acad Dermatol Venereol* 2010; 24(11):1326-1332.
38. Hillman GG, Kallinteris NL, Lu X, Wang Y, Wright JL, Li Y, et al. **Turning tumor cells in situ into T-helper cell-stimulating, MHC class II tumor epitope-presenters: immuno-curing and immuno-consolidation**. *Cancer Treat Rev* 2004; 30(3):281-290.
39. Wu C, Wang Z, Song X, Feng XS, Abnet CC, He J, et al. **Joint analysis of three genome-wide association studies of esophageal squamous cell carcinoma in Chinese populations**. *Nat Genet* 2014; 46(9):1001-1006.
40. Hussain M, Adah D, Tariq M, Lu Y, Zhang J, Liu J. **CXCL13/CXCR5 signaling axis in cancer**. *Life Sci* 2019; 227:175-186.
41. Tokunaga R, Naseem M, Lo JH, Battaglin F, Soni S, Puccini A, et al. **B cell and B cell-related pathways for novel cancer treatments**. *Cancer Treat Rev* 2019; 73:10-19.
42. Franchina DG, Grusdat M, Brenner D. **B-Cell Metabolic Remodeling and Cancer**. *Trends Cancer* 2018; 4(2):138-150.
43. Riemann D, Cwikowski M, Turzer S, Giese T, Grallert M, Schutte W, et al. **Blood immune cell biomarkers in lung cancer**. *Clin Exp Immunol* 2019; 195(2):179-189.
44. Sabado RL, Balan S, Bhardwaj N. **Dendritic cell-based immunotherapy**. *Cell Res* 2017; 27(1):74-95.
45. Wang Y, Jiang X, Wang S, Yu H, Zhang T, Xu S, et al. **Serological TK1 predict pre-cancer in routine health screenings of 56,178 people**. *Cancer Biomark* 2018; 22(2):237-247.
46. Togar T, Desai S, Mishra R, Terwadkar P, Ramteke M, Ranjan M, et al. **Identifying cancer driver genes from functional genomics screens**. *Swiss Med Wkly* 2020; 150:w20195.

47. Liu GJ, Wang YJ, Yue M, Zhao LM, Guo YD, Liu YP, et al. **High expression of TCN1 is a negative prognostic biomarker and can predict neoadjuvant chemosensitivity of colon cancer**. *Sci Rep* 2020; 10(1):11951.
48. Ketteler J, Klein D. **Caveolin-1, cancer and therapy resistance**. *Int J Cancer* 2018; 143(9):2092-2104.
49. Vijaya Kumar A, Salem Gassar E, Spillmann D, Stock C, Sen YP, Zhang T, et al. **HS3ST2 modulates breast cancer cell invasiveness via MAP kinase- and Tcf4 (Tcf7l2)-dependent regulation of protease and cadherin expression**. *Int J Cancer* 2014; 135(11):2579-2592.
50. Chen CS, Lin LW, Hsieh CC, Chen GW, Peng WH, Hsieh MT. **Differential gene expression in hemodialysis patients with "cold" zheng**. *Am J Chin Med* 2006; 34(3):377-385.
51. Nakamura T, Satoh-Nakamura T, Nakajima A, Kawanami T, Sakai T, Fujita Y, et al. **Impaired expression of innate immunity-related genes in IgG4-related disease: A possible mechanism in the pathogenesis of IgG4-RD**. *Mod Rheumatol* 2020; 30(3):551-557.
52. Codrici E, Albulescu L, Popescu ID, Mihai S, Enciu AM, Albulescu R, et al. **Caveolin-1-Knockout Mouse as a Model of Inflammatory Diseases**. *J Immunol Res* 2018; 2018:2498576.
53. Shah KN, Wilson EA, Malla R, Elford HL, Faridi JS. **Targeting Ribonucleotide Reductase M2 and NF-kappaB Activation with Didox to Circumvent Tamoxifen Resistance in Breast Cancer**. *Mol Cancer Ther* 2015; 14(11):2411-2421.
54. Yang Y, Lin J, Guo S, Xue X, Wang Y, Qiu S, et al. **RRM2 protects against ferroptosis and is a tumor biomarker for liver cancer**. *Cancer Cell Int* 2020; 20(1):587.
55. Ma C, Luo H, Cao J, Gao C, Fa X, Wang G. **Independent prognostic implications of RRM2 in lung adenocarcinoma**. *J Cancer* 2020; 11(23):7009-7022.
56. Goel S, DeCristo MJ, Watt AC, BrinJones H, Sceneay J, Li BB, et al. **CDK4/6 inhibition triggers anti-tumour immunity**. *Nature* 2017; 548(7668):471-475.

Figures

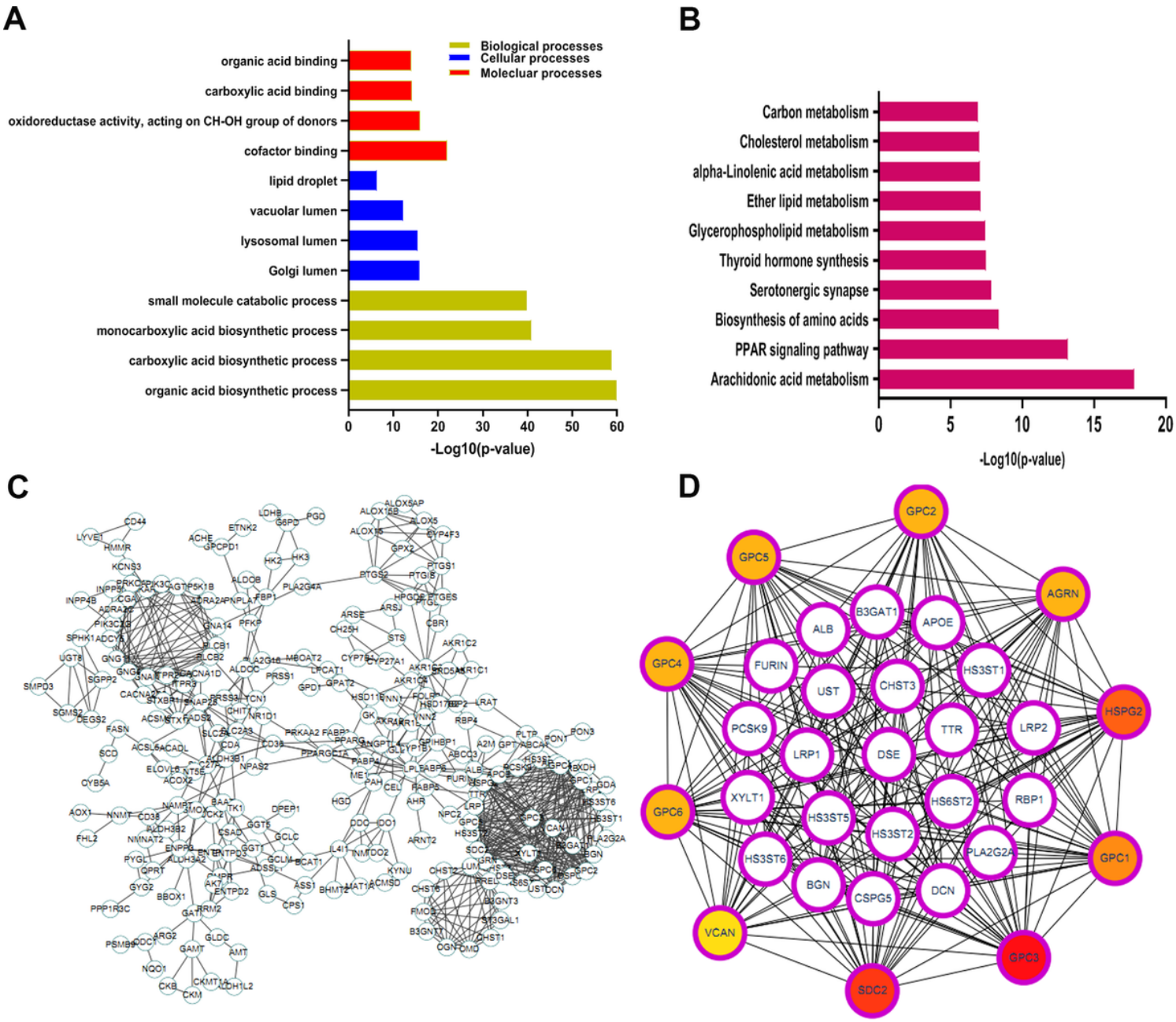

Figure 1

The Gene Ontology, KEGG pathway analysis PPI network results for immune-related metabolic genes. The GO enrichment and KEGG pathway analyses immune-related metabolic genes(A-B). (C) Interaction network constructed with the nodes with interaction confidence value >0.9. (D) The top 10 genes ordered by the number of nodes. BP: biological process; CC: cellular component; MF: molecular function; KEGG: Kyoto Encyclopedia of Genes and Genomes.

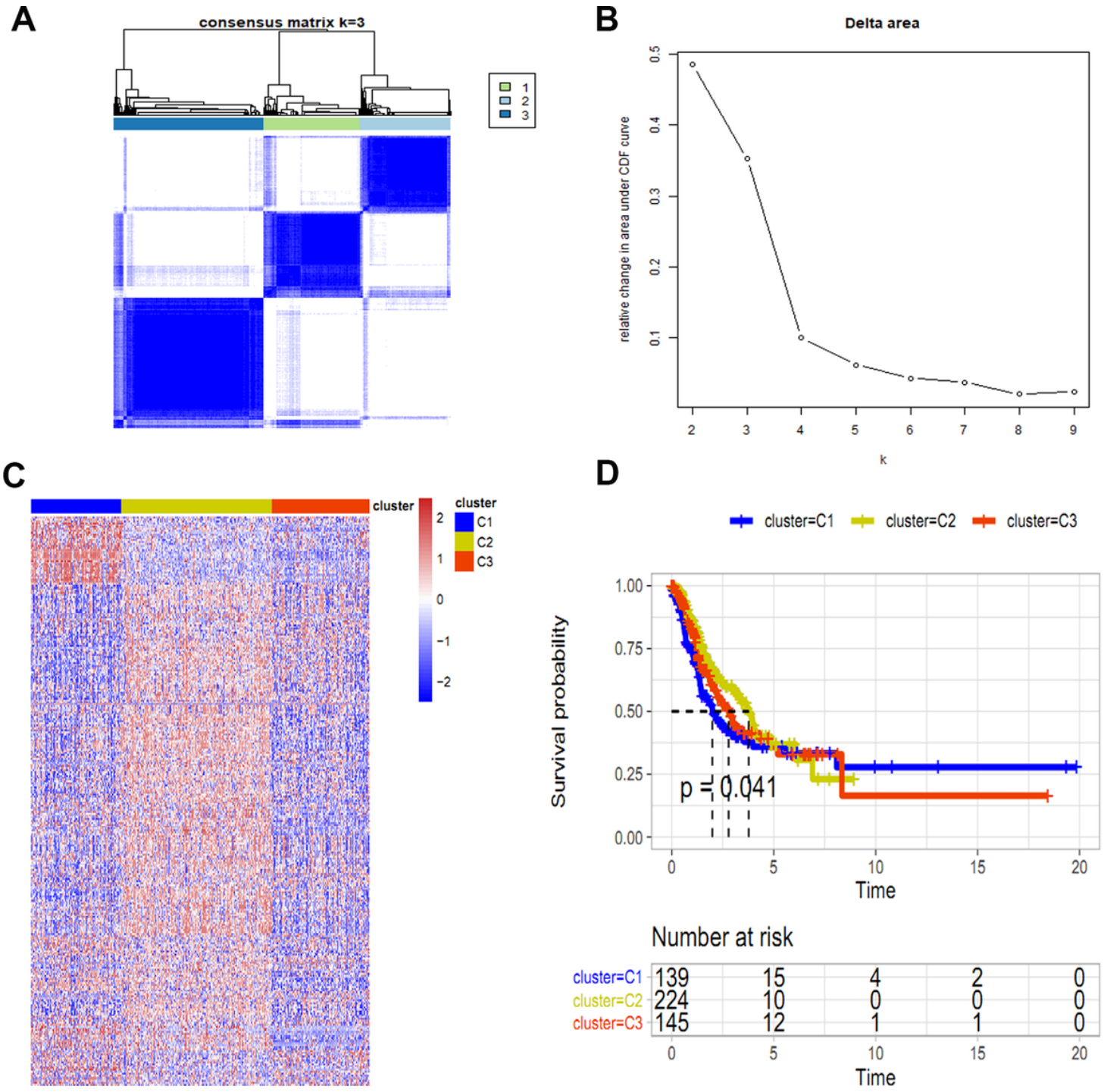

Figure 2

Consistent clustering diagram of immune-related metabolic genes. CDF (cumulative distribution function) shows that when k is 3, it is the optimal number of clusters (A-B). A heat map is drawn to show that the three clusters are among the immune-related metabolic genes(C). Survival analysis between different clusters(D).

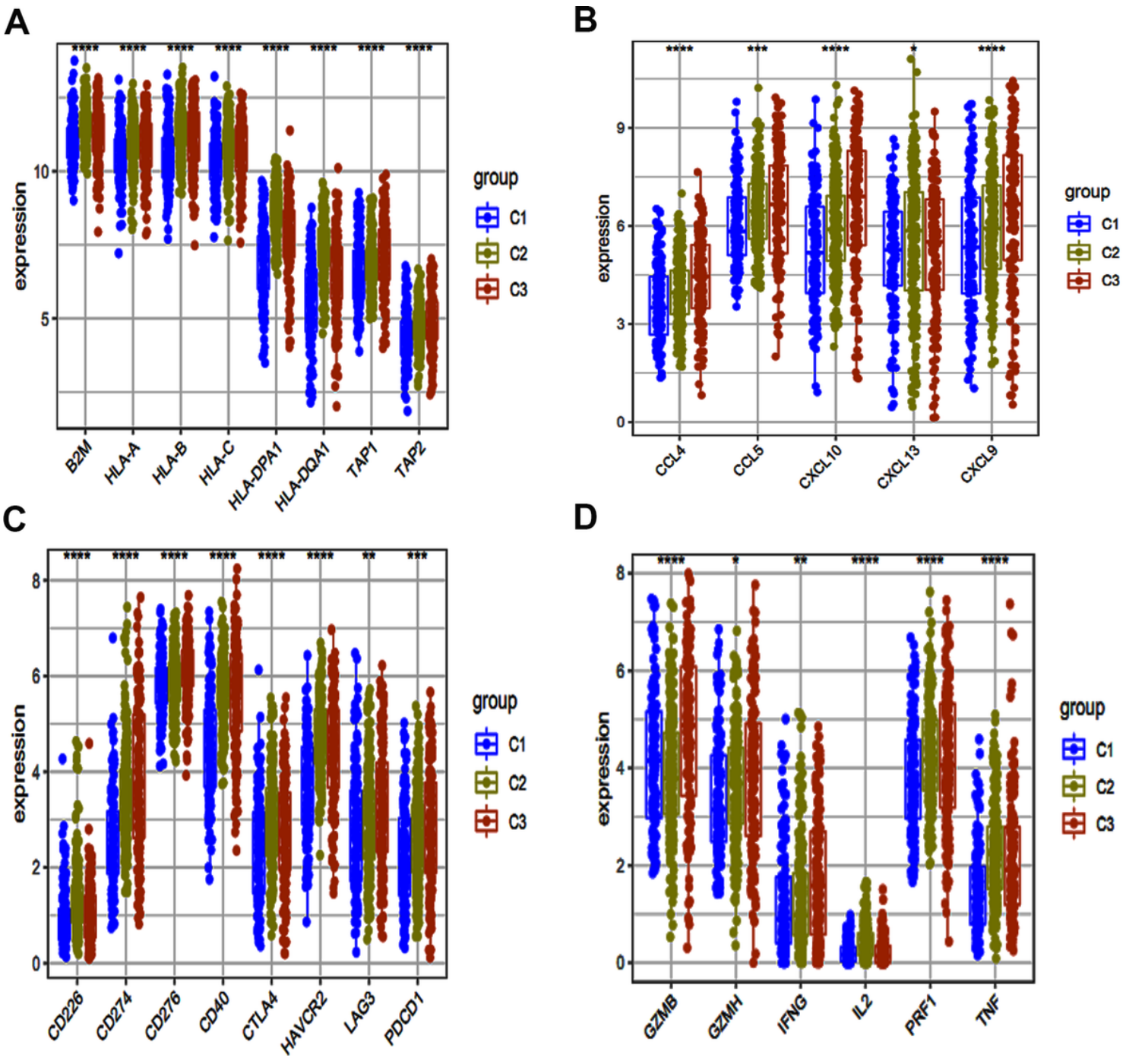

Figure 3

Box plot of immune-related gene expression between different clusters. (A-D) In the three clusters, the expression levels of multiple immune genes are compared. *, P <0.05. **, P <0.01. ***, P <0.001. ****, P <0.0001.

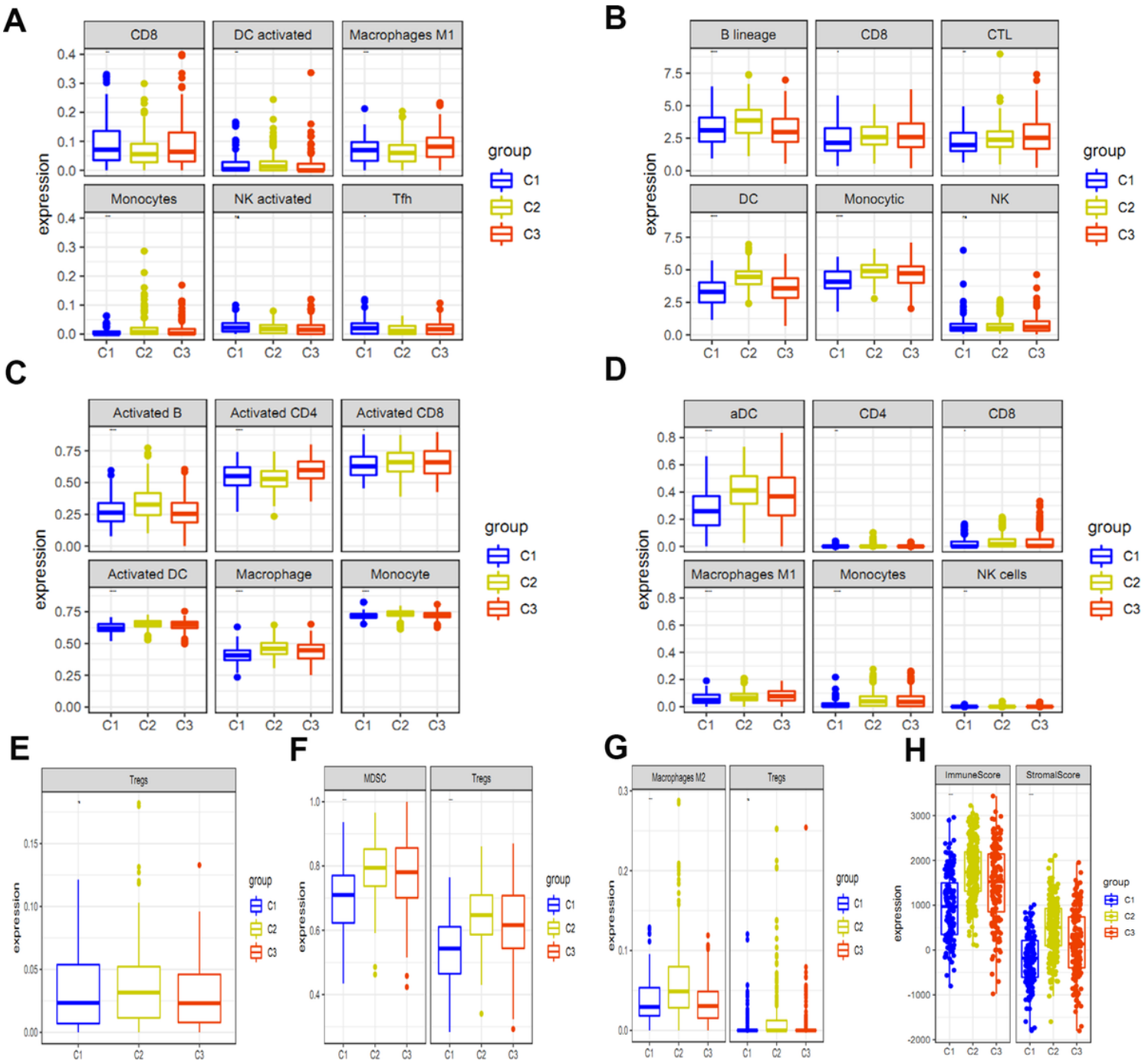

Figure 4

Immune characteristics-the expression of the level of infiltration of immune cells. (A-D) The expression of the level of immune effector cells between different clusters. (E-G) Immunosuppressive cells in different clusters. (H) Immune score and stromal score in different clusters.

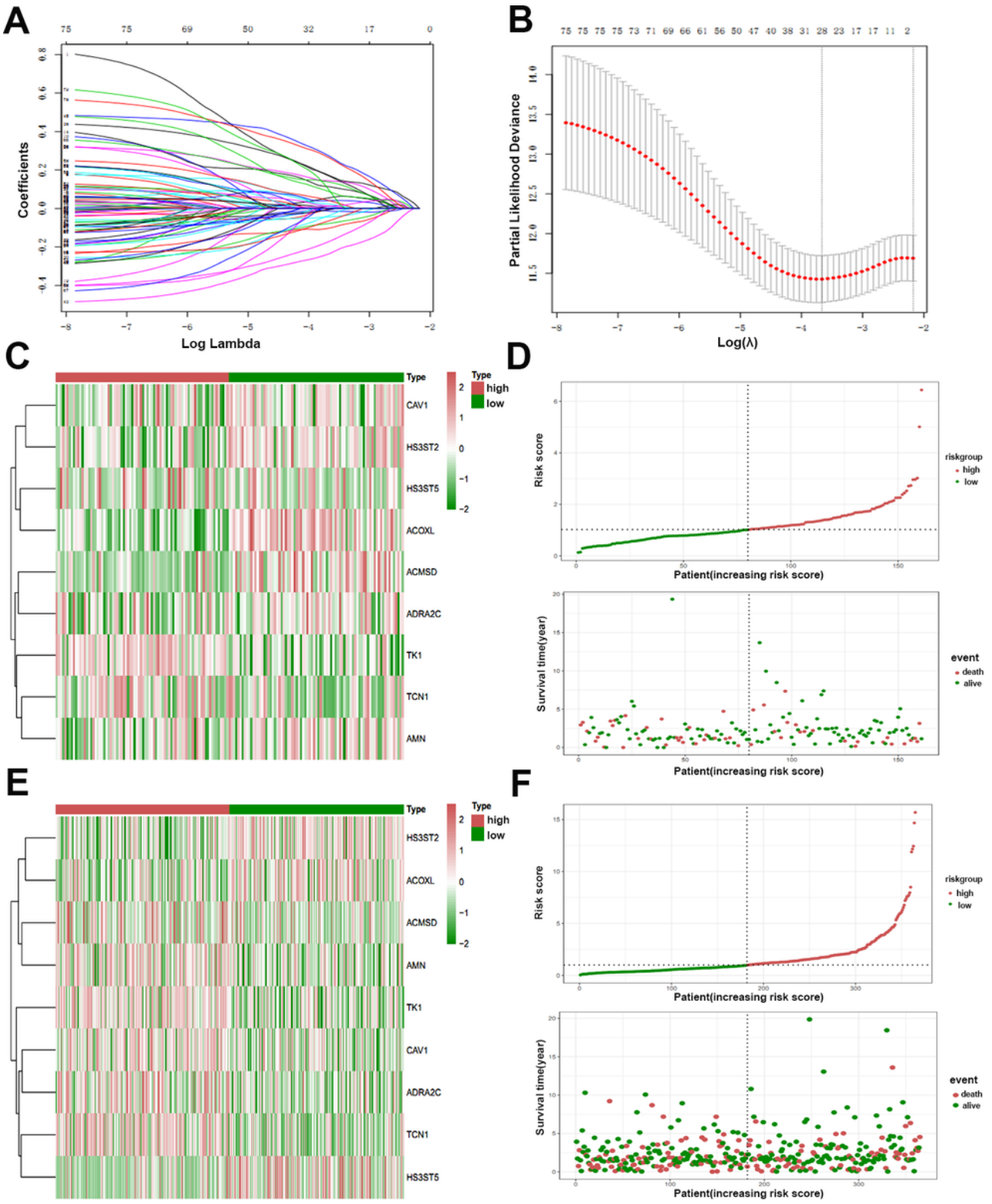

Figure 5

LASSO coefficient profiles of 9 genes were related to prognostics. (A&B) The optimal values of the penalty parameter λ were determined by ten-fold cross-validation. (C-F) The distributions of risk score of LUAD patients and the relationships between risk score and survival time were visualized.

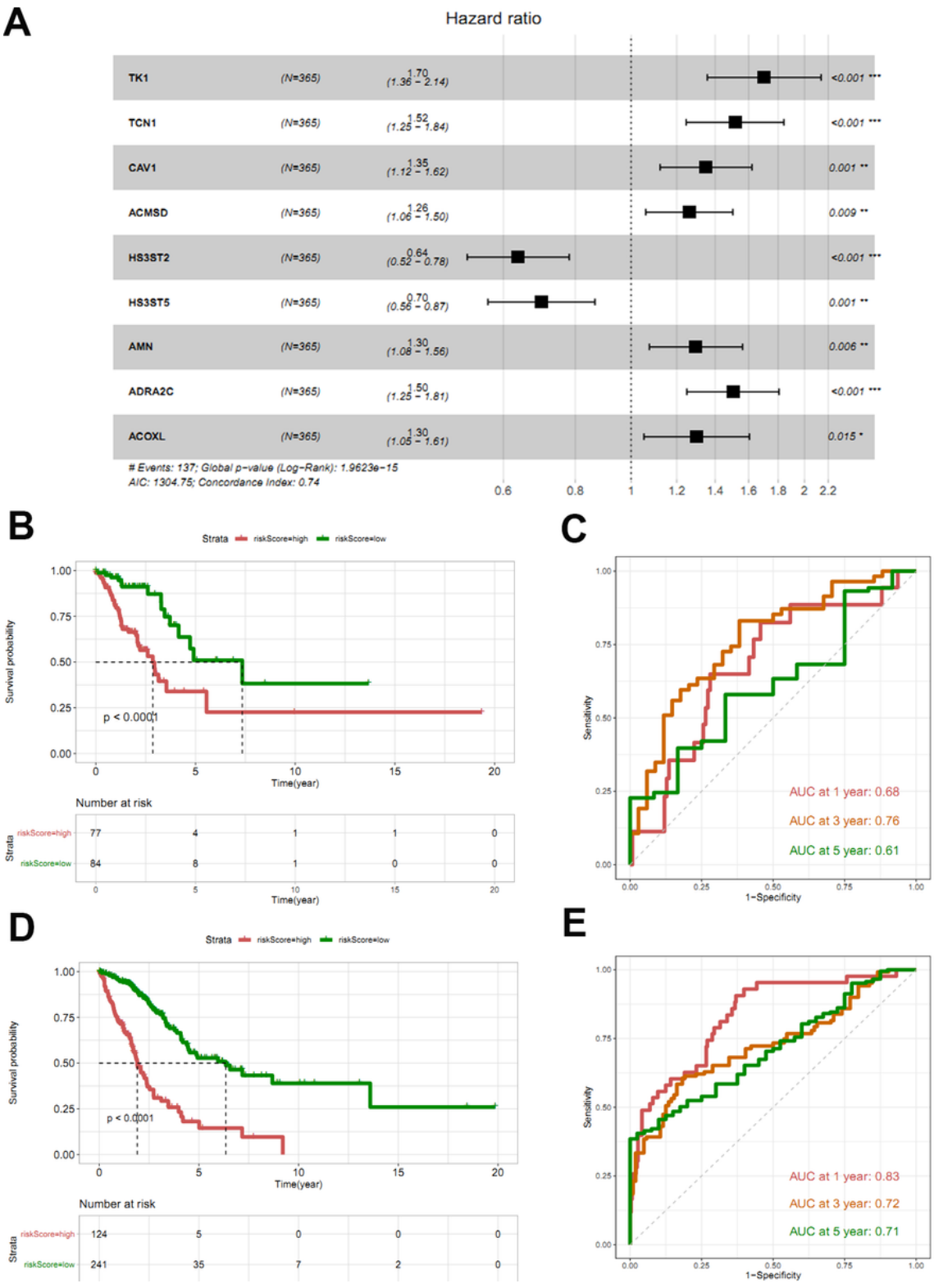

Figure 6

Construction of the hub gene prognostic model. (A) Single-factor COX analysis of 9 genes. (B&D) Kaplan-Meier curves show that OS in the low score group was significantly higher than in the high score group, and time-dependent ROC curves analysis of the prediction model(C&E).

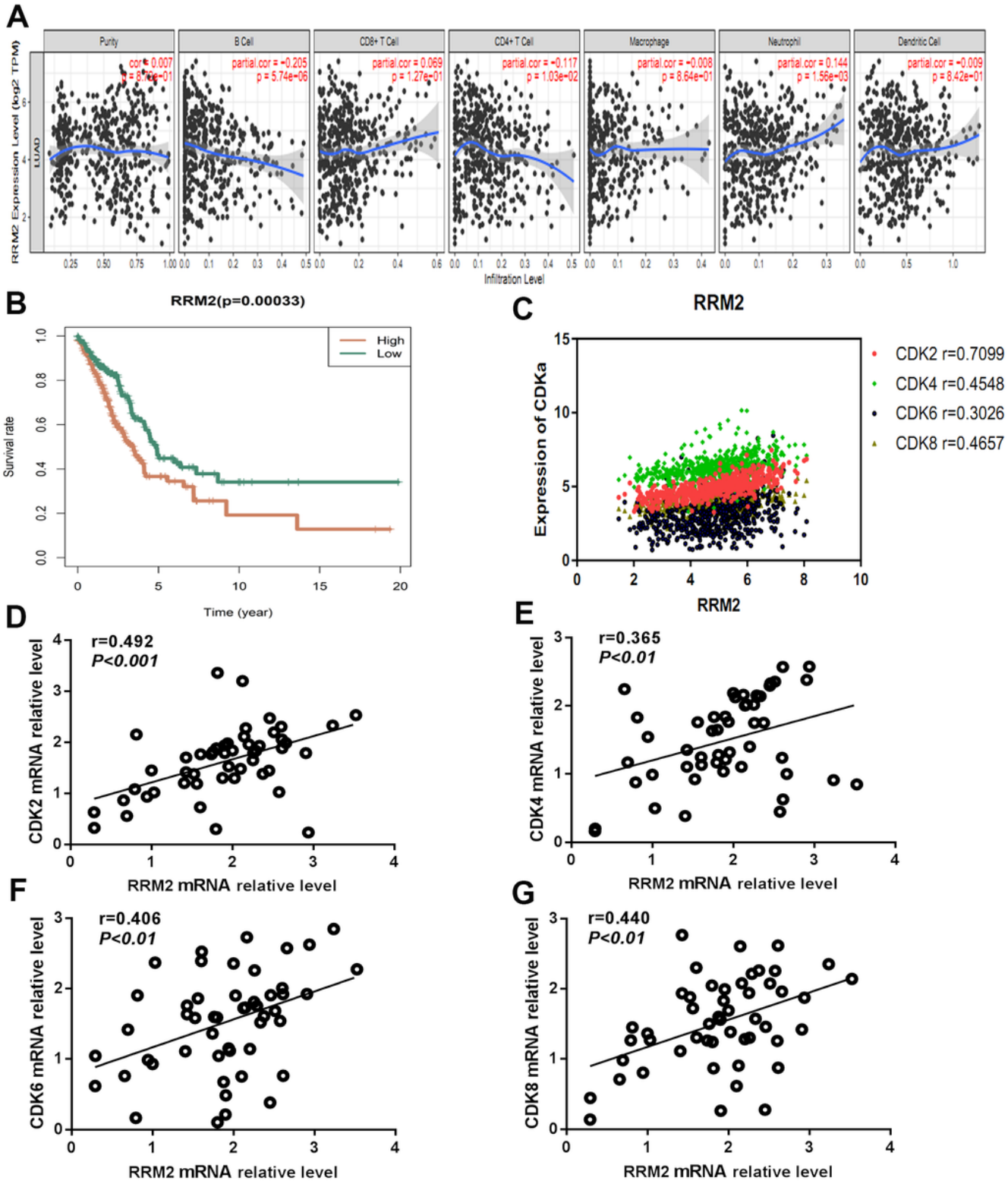

Figure 7

The relationship between RRM2 and survival time and immunity. (A-C) Correlation between RRM2 gene and CDK family. Correlation analysis of mRNA expression levels between RRM2 and CDK2, CDK4, CDK6, CDK8 using patient-derived lung cancer samples (n = 50) (Figure 7D-G).

Supplementary Files

This is a list of supplementary files associated with this preprint. Click to download.

- SupplementaryFigure1.tif
- SupplementaryFigure2.tif
- SupplementaryFigure3.tif
- SupplementaryFigure4.tif
- SupplementaryFigure5.tif
- Supplementarytable1.docx